



Mass sensitivity of multilayer thin film resonant BAW sensors

G. Wingqvist*, V. Yantchev, I. Katardjiev

Solid State Electronics, Uppsala University, Uppsala, Sweden

ARTICLE INFO

Article history:

Received 14 March 2008

Received in revised form 11 July 2008

Accepted 29 July 2008

Available online 5 August 2008

Keywords:

Mass sensitivity

Bulk acoustic resonator

FBAR

Sensitivity amplification

ABSTRACT

A systematic study of the mass sensitivity and its dependence on the material's properties and thicknesses in composite multilayer Thin Film Bulk Acoustic Resonators (FBAR) is presented. The Mason transmission line model has been employed in combination with the acoustic energy balance principle for the determination of the FBAR mass sensitivity. The results have been experimentally verified. Further, the mass sensitivity dependence on various parameters has been studied and correlated with wave reflection and interference within the composite structure in addition to the well-known dependence on resonator acoustic impedance and operation frequency. The mass sensitivity for both the fundamental and the second harmonic mode of operation has been studied in view of their practical relevance. In particular, sensitivity amplification induced by the presence of an on-top deposited low acoustic impedance layer has been identified for the first harmonic and its potential applicability discussed in terms of gas and in-liquid sensing. Optimized structures for both sensing applications are suggested by considering the overall sensor resolution defined by both the mass sensitivity and the FBAR performance.

© 2008 Elsevier B.V. All rights reserved.

1. Introduction

The possibility for low cost mass production of miniaturized and highly sensitive sensors has made the thin film electro-acoustic technology very attractive for various sensor applications. Thin Film Bulk Acoustic Resonators (FBARs) often operate at two orders of magnitude higher frequencies than Quartz Crystal Microbalance (QCM). The higher frequency and the smaller size result in that the boundary conditions have a much stronger effect on the FBAR performance than on the QCM performance. This will, as noted in several publications, result in a higher mass sensitivity, but in an increased noise level as well, thus moderating the gain in resolution. So far only publications of network analyzer based FBAR sensor measurements have been published in the literature [1–3] which show that the FBAR mass resolution is very similar if not better than for oscillator based QCM sensors, which in turn indicates that the FBAR could be a competitive and inexpensive alternative to the QCM. Low phase noise FBAR based integrated oscillator has recently been presented, which further strengthen the expectations of the FBAR sensors fabricated with low cost mass production processes [4].

A good understanding of the factors influencing the mass sensitivity is of significant importance for the design of FBAR sensors. Recently, a number of experimental and theoretical studies of the

mass sensitivity of different FBAR devices both operating in the shear and the longitudinal thickness excited mode [3,5–9] have been presented, where the shear mode FBAR has been utilized successfully for biosensor applications [1–3,10,11]. The studies of the mass sensitivity have, however, to the authors' knowledge, so far not been sufficiently extensive or complete and do not provide a comprehensive view of the major factors influencing the mass sensitivity. In a FBAR sensor, in contrast to the conventional QCM, the thickness of the electrodes is comparable to that of the piezoelectric film and hence cannot be neglected. The FBAR must, therefore, be considered to be a multilayer structure, where the acoustic path includes the piezoelectric film as well as an acoustically "dead" material, e.g. electrodes and additional layers such as for instance Au, which is commonly used as a suitable surface for various biochemical applications, or SiO₂ which also is used for temperature compensation [12]. QCM on the other hand to a good approximation is considered to be a single material resonator, the main exception in the literature being when a thick polymer layer is attached to the QCM sensor for enhancing selectivity in gas sensor applications.

It has been empirically shown that the FBAR mass sensitivity is affected by all the layers in the resonator structure and more specifically by their thickness and acoustic impedance. Recent studies of FBARs have indicated the existence of a sensitivity amplification effect if a layer of low acoustic impedance is added to the structure [7,8]. It has also been shown in the case of QCM that a mass sensitivity amplification can be obtained by the addition of viscoelastic layers [13] or with rigid thick layers of low acoustic impedance material [14]. However, there has not been a thorough study, to

* Corresponding author. Tel.: +46 18 471 00 00; fax: +46 18 55 50 95.
E-mail address: gunilla.wingqvist@angstrom.uu.se (G. Wingqvist).

the authors' knowledge, that shows in detail the influence of rigid non-viscous layers in composite resonator structures on the mass sensitivity, which is the subject of study in this work. The mass sensitivity is defined as the frequency change due to acoustically thin rigid layer deposited on either surface of the resonator structure, where only the mass, and not the stiffness, of the added layer influence the resonance frequency.

2. Theoretical background

At resonance in a lossless medium the peak total kinetic energy equals the peak total potential energy in the complete resonating structure [15]. For a multilayered resonator structure with N layers, including the piezoelectric layer, this means:

$$\sum_{i=1}^N E_{\text{kinetic}}^i = \sum_{i=1}^N E_{\text{potential}}^i, \quad (1)$$

where

$$E_{\text{kinetic}}^i = 2(\pi f_0)^2 \int_{\text{layer}_i} \rho_i u_i(z)^2 dz \quad (2)$$

and

$$E_{\text{potential}}^i = \frac{c_i}{2} \int_{\text{layer}_i} \left(\frac{\partial u}{\partial z} \right)^2 dz. \quad (3)$$

are the kinetic and the potential acoustic energy in each layer. Here $u_i(z)$ is the displacement amplitude in the i th layer, $i = 1, \dots, N$. z is the coordinate along the acoustic path, c_i the layer stiffness moduli, ρ_i the layer density and f_0 is the resonance frequency.

If an additional very thin layer of rigid mass is attached onto the surface of the multilayer structure above, there will be a corresponding additional term in the expression of the total kinetic energy (left hand side of Eq. (1)), but since the layer is very thin there will be practically no strain in the layer and hence the expression for the potential energy (right-hand side of Eq. (1)) will remain unaffected. The shift in resonance frequency Δf due to the thin rigid layer can easily be determined from the energy balance condition (1) applied to the perturbed system [15]. Further, the frequency change can be used for the determination of the pure mass sensitivity (S) defined as the relative frequency shift, $\Delta f/f_0$, normalized to the surface mass density of the rigid thin layer added onto surface:

$$S = \frac{\Delta f/f_0}{\rho_m t_m} = -\frac{(\pi f_0)^2 u_m^2}{U_{\text{kin}}^{\text{total}}} = -\frac{1}{2} \frac{u_m^2}{\sum_{i=1}^N \int_0^{h_i} \rho_i u_i(z)^2 dz} \quad (4)$$

where ρ_m and t_m are the mass density and thickness of the added layer, while u_m is the displacement amplitude in the added layer. It is to be noted that in the case of pure mass sensing the resonance shift is only affected by the mass density and thickness of the added layer and not by its stiffness or other acoustic properties. Hence, the sensitivity (S) will be independent of the choice of sensed material. It is reiterated that pure mass sensitivity can only be assumed when an acoustically thin layer is considered. The latter condition guarantees that the wave distribution within the resonator is almost unaffected by the layer to be sensed, which in turn determines negligible stress levels inside the latter. Thus, the particle displacement can be accepted uniform inside the sensed layer, i.e. $u_m(z) = u_m$.

The conventional QCM is often considered to be a *single material resonator* where the structure consists of one homogeneous piezoelectric slab only; i.e. electrodes and other additional layers including the sensed one can be neglected. Under these conditions

Eq. (4) can be written in a simplified form known as the Sauerbrey equation:

$$S = -\frac{2f_0}{\rho_r V_r} \quad (5)$$

where ρ_r and V_r are the density and acoustic wave velocity of the piezoelectric crystal respectively. It is seen, for a single material resonator that the sensitivity is directly proportional to the frequency of operation and inversely proportional to the resonator acoustic impedance $Z_r = \rho_r V_r$. The sensitivity of a single material QCM resonator is mostly defined by the quartz slab properties and has the same value on either side. A FBAR structure, however, cannot be considered to be a single material resonator since the electrodes and other additional layers make up a significant portion of the acoustic path. The electrodes only may represent up to 30% of the resonator thickness. Then the more general treatment in Eq. (4) is required where it is clearly seen that the sensitivity strongly depends on the surface amplitude normalized to the total acoustic energy in the composite structure (i.e. on the acoustic power density at the surface) as well as the frequency. The order of the included layers as well as their acoustic properties can therefore strongly influence the sensitivity through the acoustic energy redistribution stemming from the complex interference between the waves transmitted through and reflected by the layers in the composite FBAR structure. Thus, in a geometrically asymmetrical composite FBAR structure most generally the mass sensitivity on the two sides is expected to be different.

3. Mass sensitivity analysis of composite resonator structures

From Eq. (4) it is seen that sensitivity amplification could be expected if the relative energy density at the surface is increased as a result of the acoustic energy redistribution in a composite resonator. Consider a resonator consisting of a single piezoelectric slab operating in a very low impedance media such as vacuum, air or water. Most generally, a properly chosen additional layer could trap the acoustic wave closer to the surface through constructive interference between the transmitted and reflected waves in the layer. Similar cases of energy trapping are well known in acoustics. For example, a class of shear surface waves (Love waves) is represented by a bulk shear mode trapped to the surface by the guiding effect of an additional layer with lower acoustic impedance. Most generally, the acoustic wave distribution inside the composite FBAR as well as the energy density at its surfaces depends on the acoustic impedances and thicknesses of all the layers in the structure. Commonly used layers of non-piezoelectric material in the acoustic path of a thickness excited bulk acoustic resonator are the metal electrodes as well as additional layers such as for instance gold (Au, normally used to provide a chemically suitable surface for various biochemical applications), or SiO_2 (used for temperature compensation of resonators based on piezoelectric materials having a negative temperature coefficient of frequency (TCF), e.g. AlN, ZnO) [12]. Au and SiO_2 have higher and lower acoustic impedance than AlN, respectively, and are therefore also interesting to use as case study materials for illustrating how high and low acoustic impedance layers influence the sensitivity, respectively.

The most commonly used mode of operation of FBARs is the fundamental mode in view of its high coupling, but recently the second harmonic has been successfully demonstrated to yield both full temperature compensation as well as retained coupling and Q value. Both the first and the second harmonic modes illustrated in Fig. 1 are of interest for various sensor applications.

Consequently, both the fundamental and the second harmonic mode of operation will initially be analyzed for two types of struc-

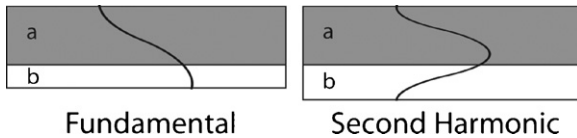


Fig. 1. Schematic illustrations of the wave distribution of the first and second harmonic mode respectively inside a two layer composite resonator consisting of one piezoelectric layer “a” and one additional solid material layer “b”. Imaginary thin electrodes for electroacoustic excitation are placed on upper and lower side of the piezoelectric layer.

tures: AlN/SiO₂/ambient and AlN/Au/ambient respectively, where ambient could be air or water, both having considerably lower acoustic impedances than both Au and SiO₂. The basic difference between the two structures is the impedance jump at the AlN/layer interface. In the first case it is from a relatively low to relatively high impedance, whereas in the second case it is the other way around. The implications are that the normalized transmitted wave in the AlN/SiO₂ case will have a relative amplitude larger than unit, while in the AlN/Au case it is smaller than 1, since the amplitude u_2 of the transmitted wave is given by:

$$\frac{u_2}{u_1} = \frac{2}{1 + z_2/z_1}$$

where u_1 is the amplitude of the incident wave, while z_1 and z_2 are acoustic impedances of the AlN and the added layer respectively [16]. In a finite structure, however, the amplitude is given by the superposition of the transmitted and reflected waves at the two interfaces together with their corresponding phases, thus the wave amplitude inside the added layer is also a function of the thickness of the added layer. To demonstrate the latter a numerical calculation with the Mason model [17] of a composite structure consisting of a semi-infinite AlN slab and an added layer of finite thickness is performed. Fig. 2 shows the peak amplitude at the surface of the added layer normalized to the incident wave amplitude as a function of the added layer thickness consisting of Au and SiO₂ respectively.

It is seen in Fig. 2 that in the case of SiO₂ (i.e. low acoustic impedance material) there are regions of constructive interference between the waves in the layer, giving rise to an increased amplitude at the surface exhibiting a maximum at a thickness of a 1/4 of a wavelength. In contrast, in the case of Au (i.e. high acoustic impedance material) the situation is reversed. This result indicates that sensitivity amplification according to Eq. (4) should be possible

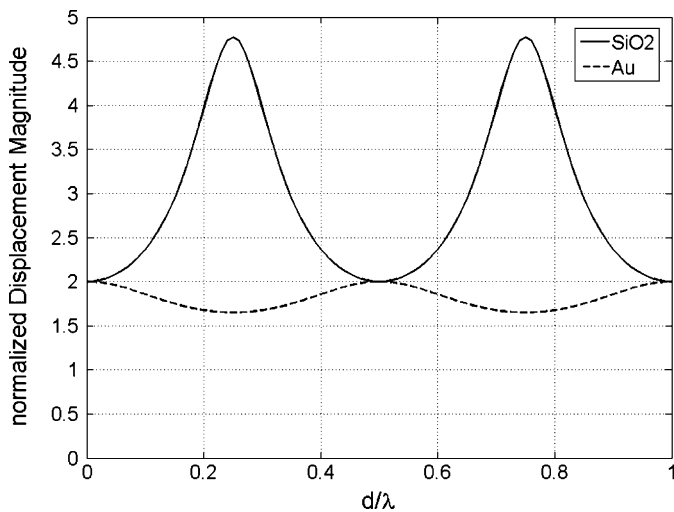


Fig. 2. The displacement magnitude at the surface of a layer of SiO₂ and Au respectively added on an infinite AlN slab, normalized to the incident wave amplitude.

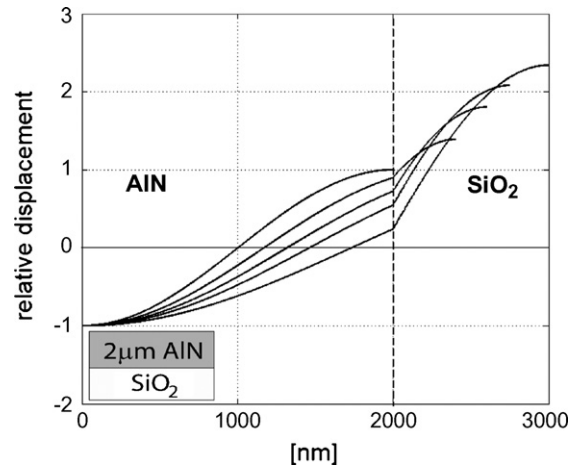


Fig. 3. Relative displacement calculated for the fundamental harmonic pure shear mode of a 2 μm AlN resonator at the moment of maximum strain, with imaginary thin electrodes on each side with an additional layer of SiO₂ of varying thicknesses.

for the first harmonic mode when adding a low acoustic impedance material to the resonator structure, due to constructive wave interference in the added layer. It is also noted in the case of the SiO₂ a minimum at 1/2 wavelength layer thickness, corresponding to an expected sensitivity minimum for the second harmonic mode at the SiO₂ side. Fig. 2 gives just a qualitative argument of the principle of possible mass sensitivity amplification due to constructive interference of acoustic waves inside an added layer only. But according to Eq. (4) one has to consider the resulting amplitude distribution inside all the layers constructing the entire resonance cavity. Consider the two types of finite structures AlN/SiO₂ and AlN/Au, respectively. The total displacement amplitude distribution for the first and second harmonic was calculated with the Mason model, for both the structures. The AlN layer was set to be 2 μm clamped between two negligibly thin electrodes where one electrode is covered with a layer of SiO₂ or Au of varying thickness. The resonator is in contact with vacuum on both surfaces. The results are given in Figs. 3–6 of the total displacement distribution at maximum strain normalized to the amplitude at the free surface of the piezoelectrically active AlN for the fundamental and the second harmonic, respectively.

As expected from Fig. 2 in the case of AlN/SiO₂ the first harmonic mode in Fig. 3 exhibits a strong increase in relative amplitude at

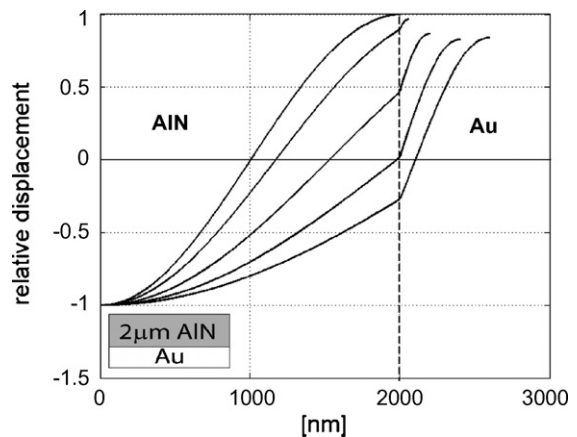


Fig. 4. Relative displacement calculated for the fundamental harmonic pure shear mode of a 2 μm AlN resonator at the moment of maximum strain, with imaginary thin electrodes on each side with an additional layer of Au of varying thicknesses.

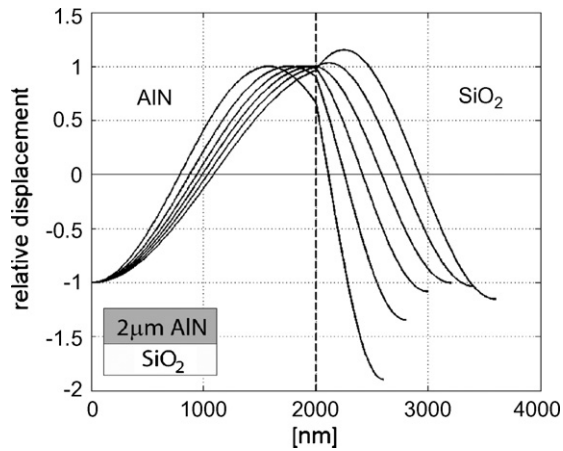


Fig. 5. Relative displacement calculated for the second harmonic pure shear mode of a 2 μm AlN resonator at the moment of maximum strain, with imaginary thin electrodes on each side with an additional layer of SiO₂ of varying thicknesses.

the SiO₂ surface with increasing SiO₂ thickness. Further, a slight decrease in the relative amplitude at the Au surface in the AlN/Au structure is observed in Fig. 4 which agrees well with Fig. 2. Figs. 5 and 6 show the calculated displacement distribution within the composite FBARs for the second harmonic of operation. The wave amplitudes at the SiO₂ and Au surfaces exhibit pronounced minima (see Fig. 5) and maxima (see Fig. 6) for certain layer thickness, respectively. The latter behavior agrees well with the expectations from the suppositions of the transmitted and reflected waves in the added layer calculated in Fig. 2. The above considerations provide some preliminary expectations about the trends in the pure mass sensitivity dependencies based on the interference of the wave, but the full description must be provided by employing Eq. (4), taking into account the wave distributions presented above as well as the frequency and impedance of the combined resonator. It is noted that the proposed algorithm for the determination of the mass sensitivity gives results, which are in excellent agreement with the mass sensitivity obtained by direct frequency shift calculations of the FBAR resonator loaded with a thin layer of arbitrary solid material [18]. The advantage of the analysis proposed above is in the direct reference to the physical phenomena causing variations in mass sensitivity here discussed. In Fig. 7 the calculated mass sensitivity for the fundamental mode on both sur-

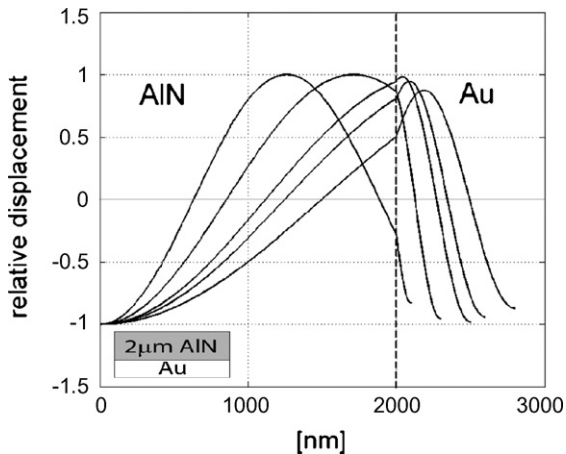


Fig. 6. Relative displacement calculated for the second harmonic pure shear mode of a 2 μm AlN resonator at the moment of maximum strain, with imaginary thin electrodes on each side with an additional layer of Au of varying thicknesses.

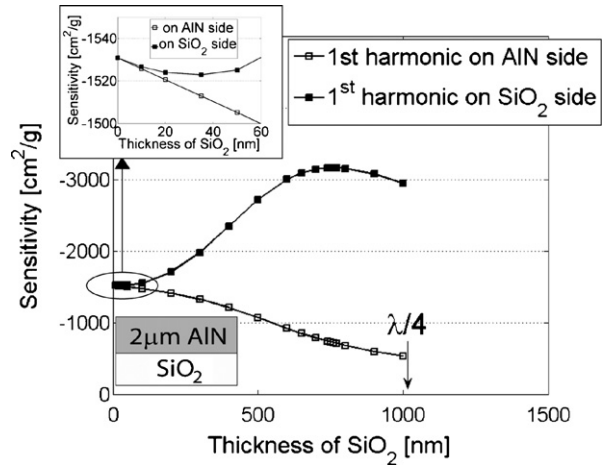


Fig. 7. Mass sensitivity calculated for the first harmonic pure shear mode of a 2 μm AlN resonator, with imaginary thin electrodes on each side with an additional layer of SiO₂ with varying thicknesses on one side. The SiO₂ thickness corresponding to a quarter wavelength ($\lambda/4$) is marked for comparison.

faces of the FBAR is shown as function of the SiO₂ thickness, for the first harmonic pure shear mode. At very small SiO₂ thicknesses the sensitivity at both sides is mostly influenced by the frequency decrease as predicted in Eq. (5). With increasing SiO₂ thicknesses the energy trapping within the SiO₂ layer shown in Fig. 2 becomes more and more pronounced, which in turn causes an increase in the mass sensitivity at the SiO₂ surface and a further decrease of sensitivity at the AlN free surface. The transition between the mainly frequency dominated and energy trapping dominated mass sensitivity regions is clearly seen at relatively small SiO₂ thicknesses. It is also seen in Fig. 7 that the maximum in mass sensitivity is not achieved at a quarter wavelength thickness of the SiO₂ layer as one might expect from Fig. 2 but rather shifted towards smaller thicknesses. This observation is explained by the constant decrease in frequency with increasing resonator thickness, which has a steady declining effect on the sensitivity. In Fig. 8 the calculated mass sensitivity on both surfaces of the FBAR is shown as a function of the Au thickness for the first harmonic pure shear mode. In this case the frequency decrease due to increased Au thickness, as well as the effective impedance increase, causes the sensitivity to decrease.

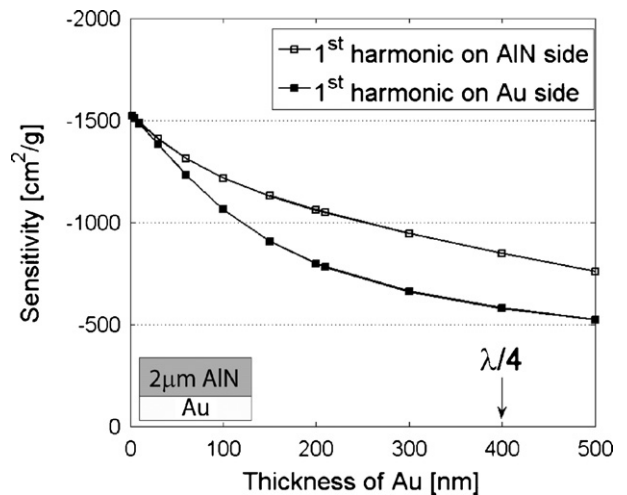


Fig. 8. Mass sensitivity calculated for the first harmonic pure shear mode of a 2 μm AlN resonator, with imaginary thin electrodes on each side with an additional layer of Au of varying thickness. The Au thickness corresponding to a quarter wavelength ($\lambda/4$) is marked for convenience.

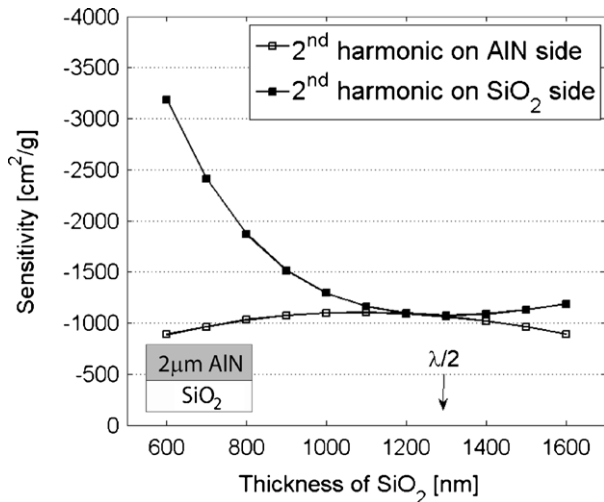


Fig. 9. Mass sensitivity calculated for the second harmonic pure shear mode of a 2 μm AlN resonator, with imaginary thin electrodes on each side with an additional layer of Au of varying thickness. The SiO₂ thickness corresponding to half wavelength ($\lambda/2$) is marked for convenience.

On the Au surface this decreased is enlarged by the addition of the decreased amplitude at this surface, due to destructive interference (Fig. 2) at the Au surface. Hence the sensitivity on the Au surface is slightly less than on the AlN free surface, where the energy trapping is slightly higher.

The results obtained for the mass sensitivity of the second harmonic in the AlN/SiO₂ and AlN/Au composite FBARs are shown in Figs. 9 and 10, respectively. In both cases the mass sensitivities at both surfaces of the FBAR become equal around the half wavelength layer thickness, where the displacement amplitudes at both surfaces are equal (see Figs. 2, 5 and 6).

Most generally, it can be concluded that the addition of a low impedance material (SiO₂) results in local maxima of the sensitivity in the case of the first harmonic, and both local minima and maxima in the case of second harmonic. Further, the addition of a high impedance material (Au) leads to a constant decrease in sensitivity. The results indicate that the main contribution to the sensitivity amplification of the first harmonic mode comes from a constructive interference of the acoustic waves in an added layer of

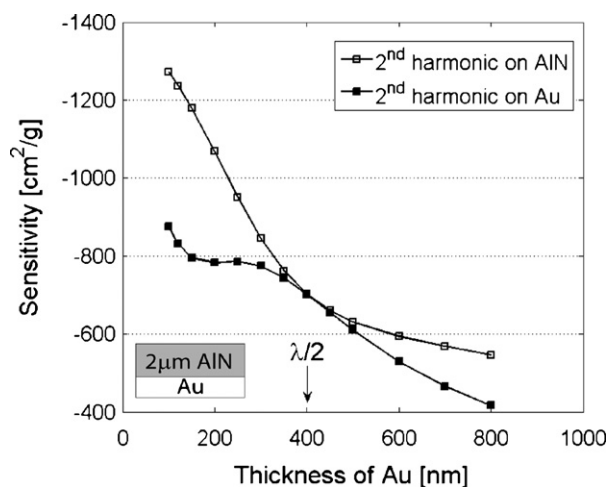


Fig. 10. Mass sensitivity calculated for the second harmonic pure shear mode of a 2 μm AlN resonator, with imaginary thin electrodes on each side with an additional layer of Au of varying thickness. The Au thickness corresponding to half wavelength ($\lambda/2$) is marked for convenience.

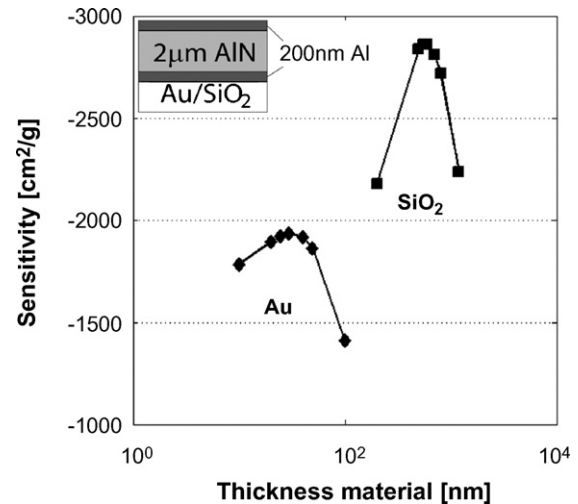


Fig. 11. Mass sensitivity calculated for the first harmonic pure shear mode of a 2 μm AlN resonator, with 220 nm Al electrodes with an additional layer of Au and SiO₂ respectively. The presented sensitivity is for the side of the resonator onto which material is added.

low acoustic impedance, giving rise to increased amplitude at the surface. It is correspondingly shown that due to non-constructive interference of the acoustic waves at the SiO₂ surface at a 1/2 wavelength and hence a decrease in the displacement amplitude, a local minimum of the sensitivity at the SiO₂ surface in the case of the second harmonic is generally expected.

The most important part of the proposed analysis is in the prediction and explanation of the possibility to achieve significant mass sensitivity amplification. Further, it should be noted that complete calculations for realistic FBAR structures consisting of 2 μm AlN, with 220 nm thick electrodes on either side showed that the addition of Al electrodes (low acoustic impedance material) will result in sensitivity amplification, equally on both sides. Thus, a sensitivity of 1620 cm²/g is obtained for a resonator with Al electrodes as compared to 1530 cm²/g for 2 μm AlN only. Including in addition a low acoustic impedance material (SiO₂) expectedly results in a further increase of the sensitivity at the layer surface (see Fig. 11). Interestingly, the addition of small thicknesses of a high acoustic material, say Au, on top of the Al electrode might still result in sensitivity amplification (see Fig. 11) provided that the effective acoustic impedance of the added Al/Au stack is smaller than that of AlN.

In many biosensor applications a thin Au layer is commonly deposited onto the resonator surface and here it is proven that by combining the Au layer with any low acoustic impedance layer (i.e. not necessarily Al as in the example above due to the high risk of bimetallic corrosion in ionic water solutions often used in biosensor applications) the added Au layer could actually result in sensitivity amplification of the sensor.

4. Experimental details and results

To verify the above predictions of sensitivity amplification, AlN thickness excited shear FBARs with varying thickness of SiO₂ were fabricated as follows. 2 μm AlN thick films with a mean tilt of the c-axis of around 25° degrees were grown by reactive sputtering [10], allowing, therefore, the excitation of the quasi shear mode. The AlN films were grown on patterned 200 nm thick Al bottom electrodes on top of Si wafers with varying thicknesses of thermally grown oxide. The oxide thickness has been varied between 0 and 1.55 μm. The active areas of size 300 μm × 300 μm were then defined by 200 nm thick Al top electrodes. For more fabrication pro-

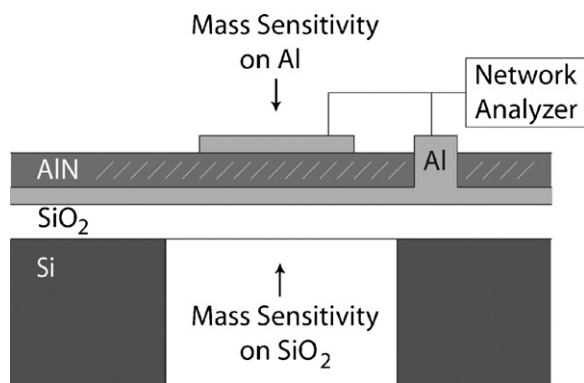


Fig. 12. Schematic illustration of the FBAR structure used in the experimental study. The piezoelectric active AlN layer is 2 μm thick, the Al electrodes are 200 nm thick and the SiO₂ layer has a thickness varying between 0 and 1.55 μm . Al₂O₃ was deposited in incremental steps on the top electrode (Al side) and on the SiO₂ side for studying the mass sensitivity on each side respectively.

cess details see previous publications [10]. A schematic illustration of the fabricated structure is shown in Fig. 12.

A well controlled reactive sputtering process was then used to repeatedly deposit 2 nm of Al₂O₃ onto the surface of various resonators and measure the frequency shift after each deposition, both the Al electrode and the SiO₂ surface were used as sensor surfaces. The electrical measurements were performed using a HP 8720D network analyzer. The parallel resonance frequency was used in the measurements since the measurement procedure demanded repeated probing of the devices and the parallel resonance frequency less sensitive to variations in the parasitic contact resistance (electrode scratching).

Four depositions of 2 nm Al₂O₃ were performed using a well-controlled reactive sputtering process onto the SiO₂ or Al surface of Al/AlN/Al/SiO₂ composite FBAR structures with varying SiO₂ thicknesses. The corresponding frequency shift of the parallel resonance frequency was measured after each deposition. The average mass sensitivity was then derived for each device and is shown in Fig. 13. For comparison, complementary calculations were performed, using 2 μm thick AlN with 25° tilted *c*-axis sandwiched between two 200 nm thick Al electrodes and SiO₂ with varying

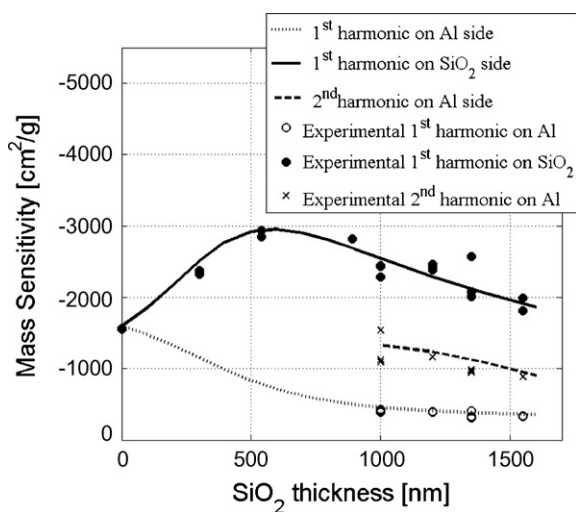


Fig. 13. Experimentally measured mass sensitivities of the first and second harmonic for various Al/AlN/Al/SiO₂ composite FBAR devices with varying SiO₂ obtained by repeated depositions of 2 nm thick Al₂O₃ on the Al and the SiO₂ respectively. Calculations are presented together with the experimental for comparison.

thickness. The calculated sensitivities are represented by the continuous lines in Fig. 13 together with the experimental points for each particular case.

As seen from Fig. 13 the agreement between theory and experiment is excellent. It does experimentally demonstrate the existence of a maximum in the sensitivity with varying SiO₂ thickness for the first harmonic, in addition to the more constant sensitivity for the second harmonic mode. In addition the experiment also clearly demonstrates the expected difference in sensitivity between the two sides of the Al/AlN/Al/SiO₂ structure. The above experiment was performed in air.

5. Sensitivity versus sensor resolution

A high resolution and well specified sensitivity of a final sensor is of substantial importance. The figure of merit (FOM) determining the noise equivalent mass resolution of oscillator based QCM sensors is often defined as [3]:

$$\text{FOM} = \frac{f_0}{QS} \quad (6)$$

where Q is the quality factor of the oscillator and S is the mass sensitivity. It is seen that an improved resolution is obtained if the sensitivity increases at the same time as the frequency of operation decreases, which is in fact confirmed by the above calculations and experimental results, where sensitivity amplification accompanied by frequency downshift of the fundamental harmonic is achieved by adding of a low impedance layer. Thus the FOM can be substantially improved by optimizing the design so that the resonator operates under sensitivity amplification conditions. Further, using SiO₂ as a low impedance layer can bring about temperature compensation of the device, which additionally improves the sensor performance [12]. On the other hand, as illustrated in Fig. 14 the sensitivity amplification normally comes at the expense of reduced coupling. At maximum sensitivity the coupling decreases by almost 40%. The latter is not crucial for gas sensing application since acoustic sensors are typically part of an oscillator circuit which can even benefit by the increased FBAR motional resistance due to electromechanical coupling deterioration. It is noted that even so the coupling is more than sufficient for gas sensing applications.

However, for in-liquid FBAR operation or biosensor applications the improved energy trapping to the sensing surface leads not only

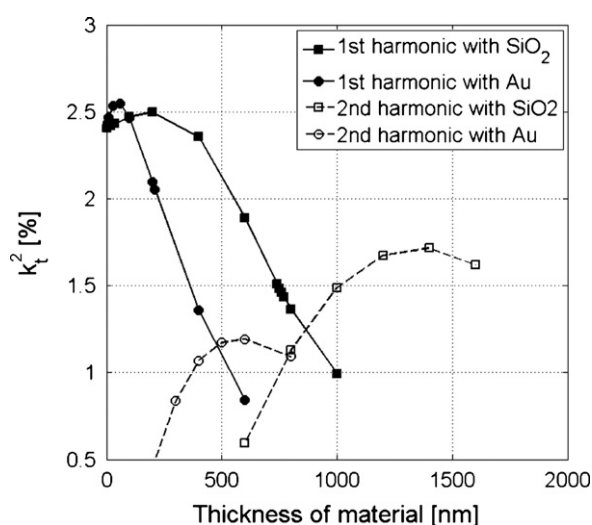


Fig. 14. Electromechanical coupling calculated for the first and second harmonic pure shear mode of a 2 μm AlN resonator, with an additional layer of various thicknesses of Au and SiO₂ respectively.

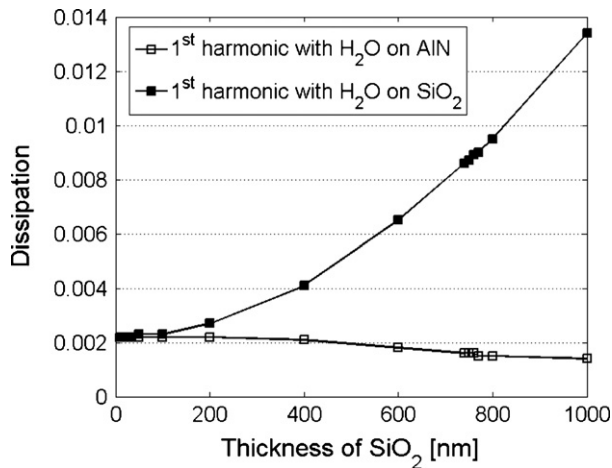


Fig. 15. Dissipation due to a liquid (water) load on one side of a 2 μm AlN resonator, calculated for the first harmonic pure shear mode of, with an additional SiO_2 layer of various thicknesses.

to an increased mass sensitivity but also to enhanced energy dissipation due to the viscous load. The latter is clearly demonstrated in Fig. 15 where the calculations are done with the one-dimensional Nowotny–Benes model [18]. All materials contained in the FBAR structure are considered to be lossless, only dissipation due to liquid load is considered. Validity of the NB calculations for liquid with various viscosities has been verified elsewhere [2].

The dissipation D has been calculated from the slope of the impedance phase Φ :

$$D = (Q_L)^{-1} = \left(0.5fr \left. \frac{\partial \Phi}{\partial f} \right|_{fr} \right)^{-1} \quad (7)$$

where Q_L is the loaded by water composite FBAR and fr is the resonant frequency.

Clearly, the mass sensitivity amplification condition will lead to an increased dissipation, which in turn leads to a deterioration of the sensor performance in terms of noise. On the positive side, this effect can be used for designing viscosity sensors for measuring very low viscosities. Further, when highly viscous liquids are to be measured the reduction of the electromechanical coupling can additionally induce performance deterioration [2]. Obviously,

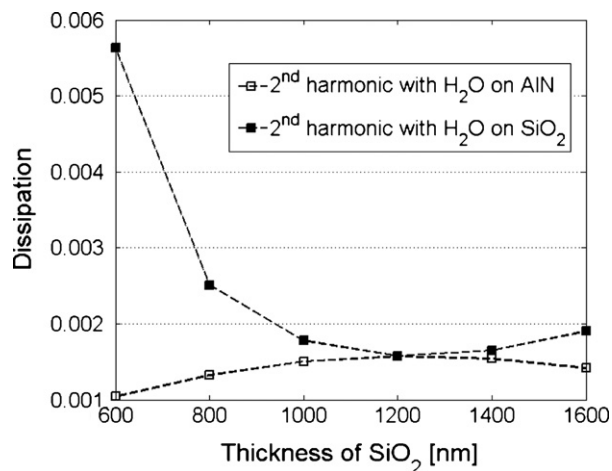


Fig. 16. Dissipation due to a liquid (water) load on one side of a 2 μm AlN resonator, calculated for the first harmonic pure shear mode of, with an additional SiO_2 layer of various thicknesses.

in liquid FBAR sensors should be designed on a trade-off basis where optimum sensitivity versus acceptable dissipation is to be chosen for the specific viscosity of the intended application. A very promising approach for designing in-liquid FBAR sensors, based on the second harmonic operation, has recently been proposed [12]. In the latter approach low dissipation levels (Fig. 16) are combined with stable and well-defined sensitivity as a function of the SiO_2 thickness (see Fig. 9) which at the same time provides a practically zero temperature coefficient of frequency.

6. Conclusions

The possibility for mass production of miniature, low cost and highly sensitive sensors has made the thin film electro-acoustic technology very attractive for various sensor applications. Earlier publications of network analyzer based measurements show that the mass resolution of the Thin Film Bulk Acoustic Resonator is similar to that for the oscillator based QCM sensors, indicating that the FBAR could be a competitive and inexpensive alternative to the QCM [1–3]. Shear mode FBAR has successfully been utilized for biosensors applications [1,3,11]. Low phase noise FBAR based integrated oscillator has recently been presented, which further strengthens the expectations of the FBAR sensors fabricated with low cost mass production processes [4].

A high resolution and well specified sensitivity of a final sensor is of substantial importance. One of the most costly steps in sensor production is the final calibration and testing of the devices, which means that an efficient mass production depends not only on the final sensor performance but also on the device sensitivity and tolerance towards deviations in the fabrication processes; i.e. the expected yield.

Systematic theoretical studies of the mass sensitivity of both composite and non-composite FBAR resonators have been performed. It has been theoretically predicted and experimentally demonstrated that the inclusion of a layer with a low acoustic impedance (lower than the piezoelectric material) in a FBAR sensor results in an enhancement of the mass sensitivity, which passes through a maximum for the 1st harmonic fundamental mode. The above enhancement is observed on the surface of the added layer and is complemented by a corresponding decrease in sensitivity on the opposite side. With respect to the 2nd harmonic the maximum is observed on the opposite side while the sensitivity on the added layer surface goes through a corresponding minimum. Finally, for a realistic FBAR resonator with non-negligible Al electrodes operating at the 1st harmonic the sensitivity exhibits a maximum for both high and low impedance of the added layer. In all cases the sensitivity amplification is argued to be a direct consequence of the interference pattern in the added layer formed as a result of the superposition of the reflected and incident waves.

The measurements are in excellent agreement with theoretical predictions.

From the above results it is concluded that if temperature compensation of AlN FBARs with an additional layer of SiO_2 is desired, then, for gas sensor applications, it is beneficial the resonator to be operated in the first harmonic, since sensitivity amplification together with a decreased frequency of operation could be obtained, while a sufficient Q value is retained. However, for in-liquid biosensors the sensitivity amplification gained from the additional low impedance layer for the first harmonics will be lost due to the substantial loss in electromechanical coupling and enhanced dissipation when in contact with a liquid. The second harmonic, which previously has been temperature compensated with retained coupling [12], will have about half the mass sensitivity of the non-composite first harmonic, but the dissipation in liquids is only one third of that of the latter, resulting in an overall gain in

resolution. It is also demonstrated that both the mass sensitivity and the dissipation of the second harmonic mode are rather insensitive towards small variations in the SiO₂ thickness rendering such devices suitable for mass fabrication.

Acknowledgements

This work is supported by the EU Biognosis project and by Vinova through the WISENET Center of Excellence.

References

- [1] G. Wingqvist, J. Bjurström, L. Liljeholm, I. Katardjiev, A.L. Spetz, Shear mode AlN thin film electroacoustic resonator for biosensor applications, in: IEEE Sensors, Irvine, CA, USA, 2005, p. 4.
- [2] G. Wingqvist, J. Bjurström, L. Liljeholm, V. Yantchev, I. Katardjiev, Shear mode AlN thin film electro-acoustic resonant sensor operation in viscous media, Sensors and Actuators B: Chemical 123 (2007) 466–473.
- [3] J. Weber, W.M. Albers, J. Tuppurainen, M. Link, R. Gabl, W. Wersing, M. Schreiter, Shear mode FBARs as highly sensitive liquid biosensors, Sensors and Actuators A: Physical 128 (2006) 84–88.
- [4] M. Norling, J. Enlund, I. Katardjiev, S. Gevorgian, A 2 GHz oscillator using a monolithically integrated AlN TFBAR, in: International Microwave Symposium, Atlanta, Georgia, 2008.
- [5] H. Zhang, E.S. Kim, Micromachined acoustic resonant mass sensor, Journal of Microelectromechanical Systems 14 (2005) 699–706.
- [6] R.P. O'Toole, S.C. Burns, G.J. Bastiaans, M.D. Porter, Thin aluminum nitride film resonators. Miniaturized high sensitivity mass sensors, Analytical Chemistry 64 (1992) 1289.
- [7] S. Rey-Mermet, R. Lanz, P. Muralt, Bulk acoustic wave resonator operating at 8 GHz for gravimetric sensing of organic films, Sensors and Actuators B: Chemical 114 (2006) 681–686.
- [8] R. Gabl, H.D. Feucht, H. Zeininger, G. Eckstein, M. Schreiter, R. Primig, D. Pitzer, W. Wersing, First results on label-free detection of DNA and protein molecules using a novel integrated sensor technology based on gravimetric detection principles, Biosensors and Bioelectronics 19 (2004) 615–620.
- [9] M. Benetti, D. Cannat, F. Di Pietrantonio, V. Foglietti, E. Verona, Microbalance chemical sensor based on thin-film bulk acoustic wave resonators, Applied Physics Letters 87 (2005) 173504.
- [10] J. Bjurström, G. Wingqvist, I. Katardjiev, Synthesis of textured thin piezoelectric AlN films with a nonzero C-axis mean tilt for the fabrication of shear mode resonators, in: IEEE Transactions on Ultrasonics, Ferroelectrics and Frequency Control, vol. 53, 2006, pp. 2095–2100.
- [11] G. Wingqvist, J. Bjurström, A.C. Hellgren, I. Katardjiev, Immunosensor utilizing a shear mode thin film bulk acoustic sensor, Sensors and Actuators B: Chemical 127 (2007) 248–252.
- [12] J. Bjurström, G. Wingqvist, V. Yantchev, I. Katardjiev, Temperature compensation of liquid FBAR sensors, Journal of Micromechanics and Microengineering 17 (2007) 651–658.
- [13] R. Lucklum, P. Hauptmann, Quartz crystal microbalance: mass sensitivity, viscoelasticity and acoustic amplification, Sensors and Actuators B: Chemical 70 (2000) 30–36.
- [14] T. Nakamoto, T. Moriizumi, A theory of a quartz crystal microbalance based upon a Mason equivalent circuit, Japanese Journal of Applied Physics, Part 1 (Regular Papers & Short Notes) 29 (1990) 963–969.
- [15] D.S. Ballantine, R.M. White, S.J. Martin, A.J. Ricco, E.T. Zellers, G.C. Frye, H. Wohltjen, Acoustic Wave Sensors; Theory, Design and Physico-chemical Applications, Academic Press, 1997.
- [16] L.E. Kinsler, A.R. Frey, A.B. Coppens, J.V. Sanders, Fundamentals of Acoustics, fourth ed., John Wiley & Sons, 2000, Incorporated.
- [17] J.F. Rosenbaum, Bulk Acoustic Wave Theory and Devices, Artech House, 1988.
- [18] H. Nowotny, E. Benes, General one-dimensional treatment of the layered piezoelectric resonator with two electrodes, Journal of the Acoustical Society of America 82 (1987) 513–521.

Biographies

G. Wingqvist is a final year Ph.D. student at the Solid State Electronics Department, Uppsala University, Sweden, where he has been studying thin film piezoelectric resonator sensors based on AlN since 2004. In 2003 he earned a Master of Science in Applied Physics and Electrical Engineering at Linköping University, Sweden. The master thesis project was concerning sputter deposition and characterization of perovskite ferroelectric thin films. The current research involves development, fabrication and characterization of the AlN thin film piezoelectric resonator transducer for various sensor applications, mainly biosensors.

Ventsislav Yantchev was born in Vratza, Bulgaria, 1976. He received the M.Sc. degree in microelectronics and information technologies and the Ph.D. degree in microwave acoustics from the University of Sofia, Sofia, Bulgaria, in 1999 and 2004, respectively. During 2004–2006 Dr. Yantchev has been a postdoctoral research associate at the Department of Engineering Sciences at Uppsala University. Currently he is a senior researcher at the same department. Dr. Yantchev's current research interests are towards the analysis, design and fabrication of thin film surface, bulk and plate acoustic wave devices. He is also lecturing in graduate and undergraduate courses on microwave electroacoustic devices. URL: <http://hermes.teknikum.uu.se/~veya/>.

Dr. Ilia Katardjiev is an associate professor at the Angstrom Laboratory, Uppsala University, Sweden. His research interests are in the area of ion-solid interactions, thin film physics, microelectronics as well as electroacoustics. Among his greatest achievements is the development of the theory of surface evolution as well as the identification of the sputter-yield amplification effect. He is the Director of a number of Swedish and European research programs and leads a group with broad R&D activities in thin film electroacoustic applications, most notably passive and active microelectronic components, chemical and biochemical sensors, etc. He earned his Ph.D. in Electrical Engineering from Salford University, U.K. in 1989 and since then has been working as a research scientist and a lecturer at Uppsala University. He has published over 100 refereed papers and presented over 20 invited and plenary lectures.